

THE DEVELOPMENT OF DIRECT AGE 718  
FOR GAS TURBINE ENGINE DISK APPLICATIONS

D. D. Krueger

General Electric Company  
GE Aircraft Engines  
Engineering Materials Technology Laboratories  
Cincinnati, Ohio

Abstract

The processing trials and evaluations which led to the use of Direct Age 718 as a commercial gas turbine aircraft engine disk material are described. Initial trials performed on pancake forgings showed that high forge reductions, low forge temperatures, and heat treatment with only an age could produce very high tensile strength in Alloy 718 without degrading needed creep and stress rupture properties. As a result, trial full-scale disks were processed using this "Direct Age" technique. More extensive mechanical property testing successfully demonstrated the potential of this material for disk applications and showed that the process window was suitable for production practice. Mechanical property results for the trial pancake and disk forgings are presented and related to microstructural characteristics and processing parameters. The best combination of tensile, creep, and low cycle fatigue properties resulted from microstructures with a uniform distribution of fine recrystallized grains and a limited amount of the delta phase precipitate. The results of investigations performed to study fatigue behavior, aging response, and heat treatment effects are also discussed.

## Introduction

Three versions of wrought Alloy 718 are currently used by GE Aircraft Engines (GEAE) in the production of gas turbine engine components (1). "Standard Processed" Alloy 718 is used for noncritical or difficult to make shapes and has an average grain size of ASTM 4-6. "High Strength Processed" Alloy 718 is used for more highly stressed components with less complex configurations and has an average grain size of ASTM 8. The third version, "Direct Age Processed" Alloy 718, achieves the highest tensile at a further expense in shape making capability. This material has an average grain size of ASTM 10, and is used in disk applications where high tensile and fatigue strength are required. The tensile strength, stress rupture, and low cycle fatigue (LCF) properties of these three Alloy 718 materials are compared in Figure 1 (1). High Strength Processed Alloy 718 (HS718), and especially Direct Age Processed Alloy 718 (DA718) show significant improvements in tensile strength and LCF properties, but exhibit lower stress rupture life in the low stress-high temperature regime.

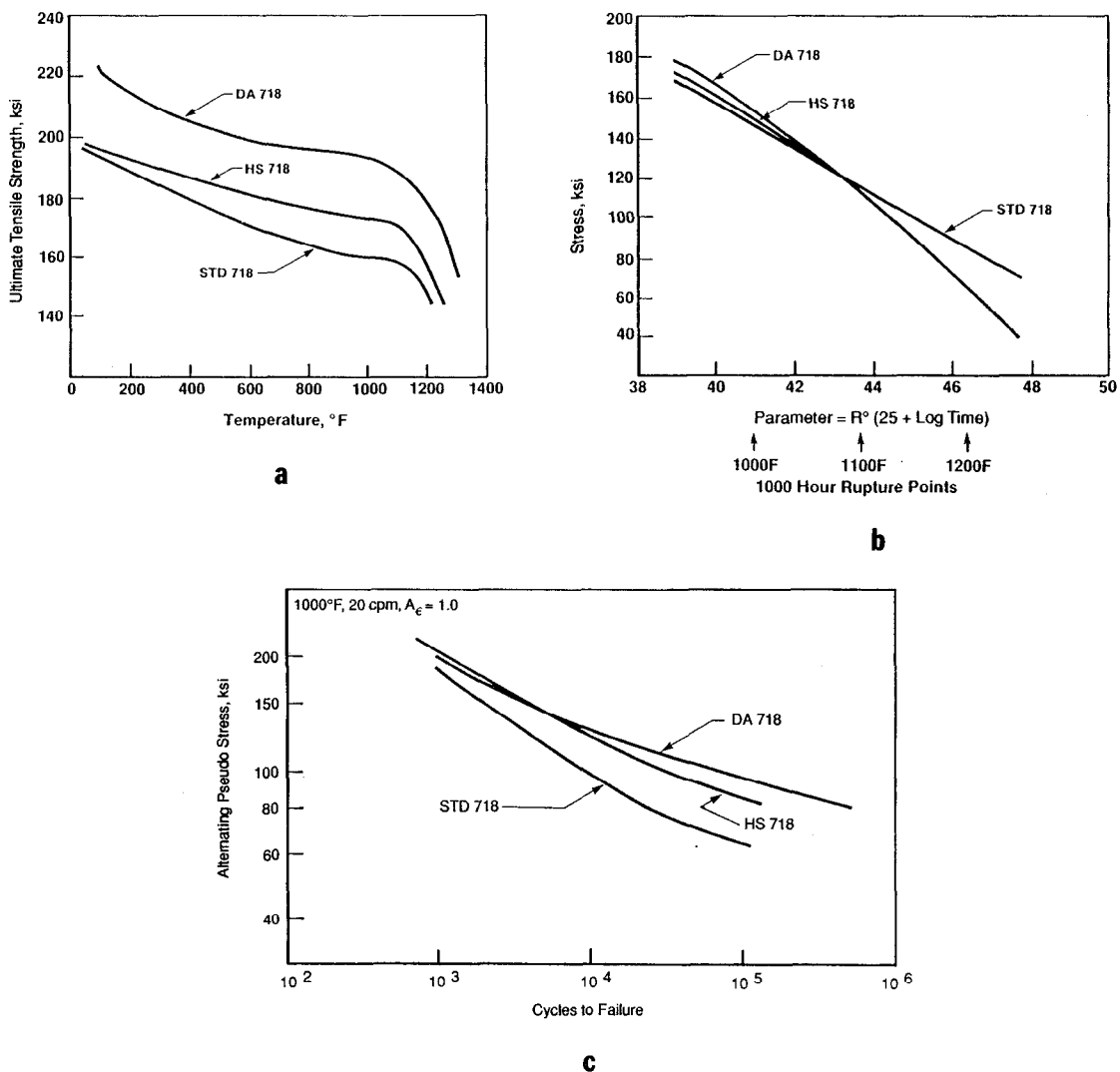


Figure 1 - Typical properties of Standard Processed, High Strength Processed, and Direct Age Processed Alloy 718; (a) ultimate tensile strength, (b) stress rupture, and (c) 1000°F low cycle fatigue (1).

As a result of its higher tensile strength, improved LCF capability, and good low temperature creep-stress rupture properties, DA718 has played a significant role in the success of advanced commercial engines developed by GEAE during the 1980's. For compressor and turbine disk applications, this material met the required property improvements and offered a low cost alternative to powder metallurgy Rene'95. The development of DA718 also extended GEAE's widespread usage of a disk alloy composition considered to have a low strategic element content.

The potential of DA718 for disk applications was first recognized during the late 1970's when GEAE and the Wyman Gordon Company performed a feasibility study on pancake forgings. After several processing trials, work to demonstrate full-scale capability was initiated using compressor disk forgings. The evaluation of these forgings helped identify the process window for DA718 and led to its current usage as a production disk material. The processing, microstructures and mechanical properties of the trial pancake and compressor disk forgings are described in this paper. Since the intent of the development effort was to improve the properties of HS718, this material has been selected for microstructure and property comparisons in the presentation of results. The work described in this paper spanned the 1977-1981 time period. Results from other subsequent parametric studies on DA718 can be found in Ref. 1.

### Physical Metallurgy of Alloy 718

The physical metallurgy of Alloy 718 has been the subject of many papers and is only briefly reviewed here. The nominal composition of the alloy is 53Ni, 19Cr, 18Fe, 3Mo, 5Nb, 1Ti, 0.5Al, 0.05C, and 0.005B (weight percent). In the fully heat treated condition, wrought Alloy 718 consists of a gamma ( $\gamma$ ) matrix,  $\gamma'$  and  $\gamma''$  precipitate phases, and small amounts of NbC carbides and TiN nitrides. Depending on the processing, delta ( $\delta$ ) phase can also be present. In rare cases, complex carbide, Laves, and other phases have been observed, but these are generally the result of poor ingot homogenization practice, abnormal heat treatments, or very long time exposure.

The major strengthening precipitate in Alloy 718 is the Ni<sub>3</sub>Nb  $\gamma''$  phase, which is coherent and has a DO<sub>22</sub> crystal structure. These precipitates are disc-shaped and have a diameter of 20-40 nm after conventional aging treatments. The  $\gamma''$  strengthening is due to coherency strains that arise during precipitation (2). A lower amount of Ni<sub>3</sub>(Al,Ti)  $\gamma'$  phase (L1<sub>2</sub> structure) is present in the alloy, and these precipitates form as spherical shaped particles with a similar or smaller diameter. The  $\gamma''$  phase begins to solution between 1550 and 1600°F, while the solvus of the  $\gamma'$  phase is somewhat lower (3). The precipitation sequence and association of the  $\gamma'$  and  $\gamma''$  phases during formation have been the subject of debate, but the differences most likely arise from variations in the amount of Ti, Al, and Nb. Studies of Alloy 718 type compositions have shown that the ratio of these elements affects the nucleation and precipitation characteristics of these phases (4).

Both the  $\gamma'$  and  $\gamma''$  phases are metastable in Alloy 718. The stable phase is Ni<sub>3</sub>Nb  $\delta$ , which is incoherent and has an orthorhombic crystal structure. This phase forms as intragranular laths along {111}, or by a cellular reaction at grain boundaries (5). Precipitation of the  $\delta$  phase is usually most pronounced in the 1700-1750°F range, and the solvus is typically near 1800°F. The  $\delta$  phase plays an important role in the control of grain size for wrought Alloy 718 since its presence can inhibit grain coarsening during processing and heat treatment.

Commercial heat treatments for wrought Alloy 718 typically consist of a 1-2h solution treatment followed by a duplex age at intermediate temperatures. Solution temperatures just below the  $\delta$  solvus are selected to dissolve the  $\gamma'$

and  $\gamma''$  phases and maintain the fine grain size developed through wrought processing. One of the common duplex age treatments consists of an 8h age at 1325°F followed by a furnace cool at 100°F per hour to 1150°F, an additional 8h age at this temperature, and air cool. This treatment will be referred to as the standard duplex age.

### Pancake Forging Trials

#### Background

Earlier work at Wyman Gordon Company (6) had shown that a high forging reduction at temperatures near the  $\delta$  solvus could significantly improve the tensile strength of Alloy 718 when combined with a modified heat treatment practice. For heat treatment modification, the conventional wrought Alloy 718 solution was omitted, and only the standard duplex age was applied. This forging and heat treatment technique later became known as the Direct Age process. As a result of the attractive strength levels, GEAE conducted two additional processing trials to determine whether full-scale disk trials were warranted. All forging work was performed by the Wyman Gordon Company.

#### Processing

Processing for the first pancake trial was based on the earlier work (6). A 12.5 inch high by 6.25 inch diameter billet (Carpenter Technology heat 95841, Table I) was prepared by solution treating the billet at 1950°F and water quenching. This dissolved all  $\delta$  phase and resulted in an average grain size of ASTM 2. Two forging operations using a 1775°F preheat and upset temperature for each were performed to obtain a pancake thickness of 5.5 inches. After quartering, two additional 1775°F forging operations were used to obtain a finish thickness of 1.5 inches. The total reduction in height for this trial was 88%. All upset operations were followed by a water quench, and insulating cloth and stainless steel sheet covers were used during the last two upsets to decrease die-work piece contact friction. Aging was performed using the standard duplex age. As discussed later, these process conditions did not provide desirable microstructures or properties, and thus modifications for a second trial were selected.

Table I. Composition of Alloy 718 Heat for First Trial Pancake Forgings (w/o)

Fe	Cr	Mo	Ti	Al	Nb+Ta	B	C	Ni
17.96	18.72	3.13	0.93	0.60	5.34	0.003	0.034	52.4

Processing for the second forging trial was designed to input a uniform grain size of ASTM 8 into the final forging operation. A 13 inch high by 6.25 inch diameter billet (Special Metals heat 95115, Table II) was upset to a 6 inch height at 1950°F, air cooled, and cut in half for further processing. After a second upset at 1825°F to 3 inches high, a slug was removed for a recrystallization study. Metallographic examination of samples exposed over the 1750 to 1825°F range showed that 1775°F produced the most uniform, refined structure. Quarter pieces were then upset at 1775°F to the 1.5 inch thickness, water quenched, and aged using the standard duplex age. Insulating cloth and stainless steel covers were again used to minimize die-work piece contact friction. Several additional forgings were also prepared using similar

conditions, but two, rather than three upsets to achieve the same total height reduction (Special Metals heat 9-5166, Table II). The processing for all second trial forgings resulted in nearly the same overall height reduction as the first trial forgings.

Table II. Composition of Alloy 718 Heats for Second Trial Pancake Forgings (w/o)

Fe	Cr	Mo	Ti	Al	Nb+Ta	B	C	Ni
18.6	17.8	2.95	0.97	0.55	5.29	0.003	0.04	53.2*
18.6	17.9	2.95	0.91	0.48	5.22	0.003	0.04	53.4**
* heat 95115		**heat 95116						

### Structure

Despite the efforts to reduce die-work piece contact friction, macrostructures of all forgings revealed evidence of coarse, unrecrystallized grains in "die chill" areas. Within the forgings, microstructures of the first trial pancakes typically consisted of a mixture of coarse unrecrystallized grains with a high aspect ratio, and extremely fine recrystallized grains about ASTM 14 in size. The structure was also heavily decorated with  $\delta$  phase owing to the multiple forging operations at 1775°F. As a result of the higher intermediate upset temperature, the second trial materials exhibited a more recrystallized structure and better grain size uniformity in the non-die chilled areas, although partially recrystallized areas were still observed. The optical micrographs of Figure 2 illustrate the range in grain structure for the second trial forgings. The average grain size in fully recrystallized areas is about ASTM 13, and these materials contained much less  $\delta$  phase than the first trial materials.

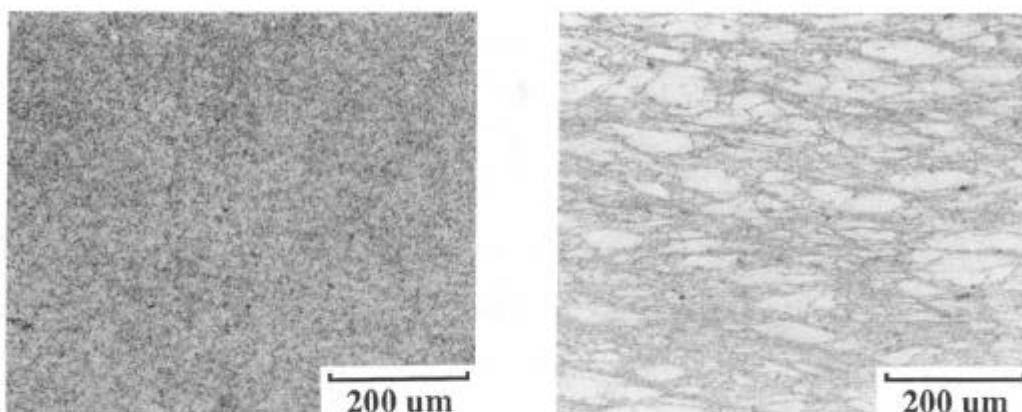


Figure 2 - Range in microstructure observed for second trial pancake forgings.

### Results and Discussion

Tensile, creep, and stress rupture properties were determined using ASTM recommended specimen geometries and test procedures. Although care was taken to machine specimens from non-die chill regions, some variability in

microstructure for each pancake was still expected. The metallographic evaluation of test specimens was used to determine actual microstructures and develop process-structure-property relationships.

Ultimate tensile and 0.2% yield strength results for all pancake materials are shown in Figure 3. Ultimate tensile strength (UTS) data typically range from 20 to 30 ksi higher than HS718 over the room temperature to 1000°F range, while the advantage at 1200°F is smaller. The improvement in 0.2% offset yield strength (YS) is even greater (30 to 40 ksi) for lower test temperatures, but the advantage again diminishes at the higher temperatures. Tensile reduction in area results for all second trial materials were found to be similar to or better than HS718, while poor low temperature ductility was evident for the first trial materials.

The study of tensile specimen microstructures revealed that grain structures varying from partially recrystallized to fully recrystallized did not have a pronounced effect on UTS or YS levels, and that lower ductility could be associated with a larger amount of the  $\delta$  phase. It was also noted that the use of two, rather than three forging operations resulted in no consistent difference in tensile properties.

Results for constant load creep and stress rupture tests performed over the 900 to 1200°F temperature range are shown in Figure 4. The creep properties are represented by the time to 0.2% total strain, and all results are presented on a Larson-Miller parameter basis. A clear distinction between the creep and stress rupture strength of the first and second trial materials is evident. The first trial pancakes exhibit lower strength at each stress level, and particularly poor behavior for low stress-high temperature (1100-1200°F) tests. Results for the second trial pancakes are much better, and similar to the capability of HS718 at all test conditions. The best creep properties were associated with a uniform recrystallized grain structure containing a low amount of the  $\delta$  phase.

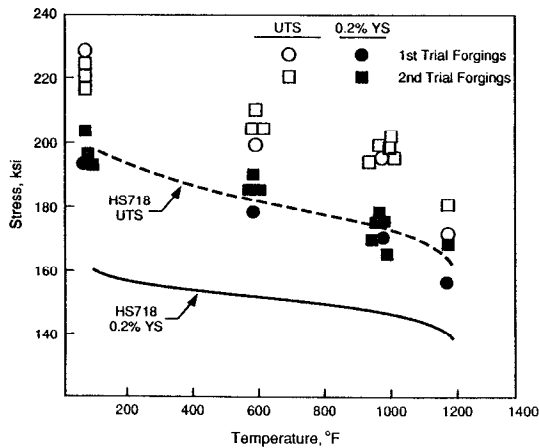


Figure 3 - Tensile data for trial pancake forgings.

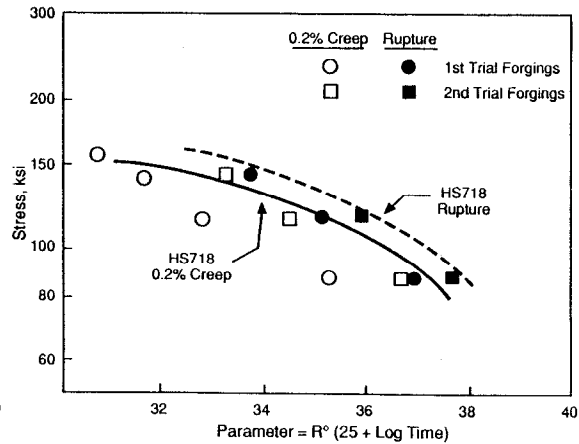


Figure 4 - Creep and stress rupture data for trial pancake forgings.

The study of process-microstructure-property relationships revealed that repeated forging at 1775°F would result in largely unrecrystallized microstructures and pronounced precipitation of the  $\delta$  phase. This method of processing was used for the first trial pancakes and associated with lower tensile ductility and creep-stress rupture strength. Due to the use of a higher forging temperature prior to the final forging operation, the second trial materials exhibited an improvement in grain structure uniformity and contained

much less  $\delta$  phase. This processing resulted in better tensile and creep-stress rupture properties. The best creep properties were associated with a uniform recrystallized grain structure containing a low amount of the  $\delta$  phase. It was also observed that reducing the number of forging steps did not affect tensile properties.

### Compressor Disk Trial

#### Overview

The pancake forging trials showed that the Direct Age process could improve the tensile strength of HS718 without degrading creep and stress rupture properties. As a result, full size hardware processing trials were performed using a compressor disk configuration. All forging work was conducted by the Wyman Gordon Company, and their evaluation included initial structure and property characterization. Investigations at GEAE were performed to more fully characterize the structure, evaluate a wide range in mechanical properties, and study aging response and heat treatment effects.

#### Processing

Based on results of the pancake trials, a process matrix for the compressor disk forgings was designed. Process variables were selected to define the window for production practice, and included variations in forging temperature, reduction, transfer time, quench procedure, and billet grain size.

To promote the development of a fine, recrystallized grain structure, 8 inch diameter billet (Special Metals heat 96225, Table III) with an average grain size of ASTM 6 was selected for the compressor disk forging trials. A metallographic study was performed to determine the  $\delta$  solvus temperature of the billet and guide the selection of forging temperatures. The optical micrographs of Figure 5 show that considerable  $\delta$  phase has precipitated as intragranular laths in the billet microstructure after a 1750°F/2h exposure, while negligible  $\delta$  phase is present after a 1800°F/2h exposure. The  $\delta$  solvus temperature is thus about 1775°F. Eight disk forgings were processed from 12 inch high multiples using two forging operations to achieve the shape illustrated in Figure 6. In all cases, insulating cloth and warm dies were used to improve structure uniformity and minimize die-work piece contact friction. The first upset was always followed by an air cool, while the second upset was typically followed by a water quench. Typical transfer times from furnace-to-press or press-to-water quench were about 1 minute.

Table III. Composition of Alloy 718 Heat for Compressor Disk Forgings (w/o)

Fe	Cr	Mo	Ti	Al	Nb+Ta	B	C	Ni
19.48	18.72	2.91	0.97	0.67	5.30	0.004	0.038	53.4

Table IV lists the process parameters for each forging. Forging A was designated as the reference material since these parameters were selected on the basis of the pancake trial results. The forging conditions for this disk consist of a 60% height reduction at 1875°F and a 75% height reduction at 1800°F (90% total reduction). The final upset temperature is just above the  $\delta$  solvus. The other forgings had variations in quench procedure (forgings B and C),

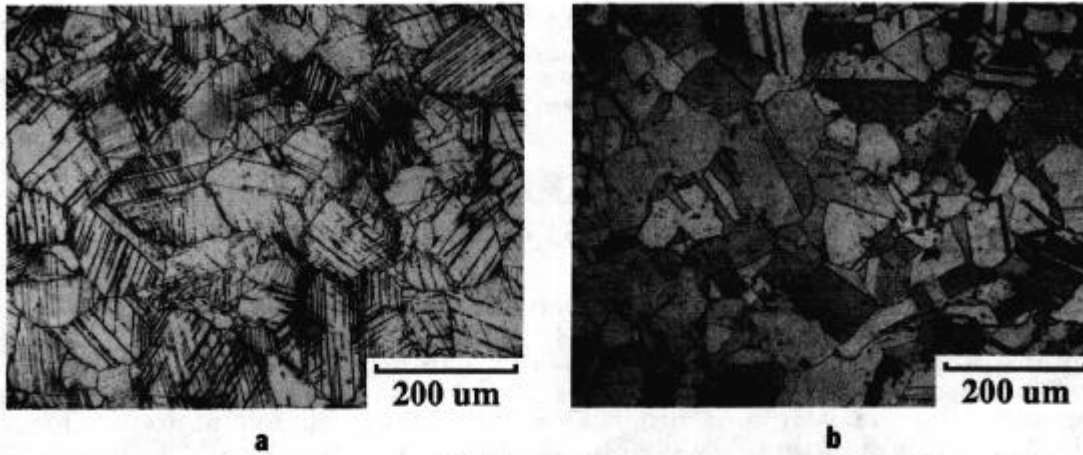


Figure 5 - Microstructure of billet used for compressor disks after a 2h exposure at (a) 1750°F and (b) 1800°F.

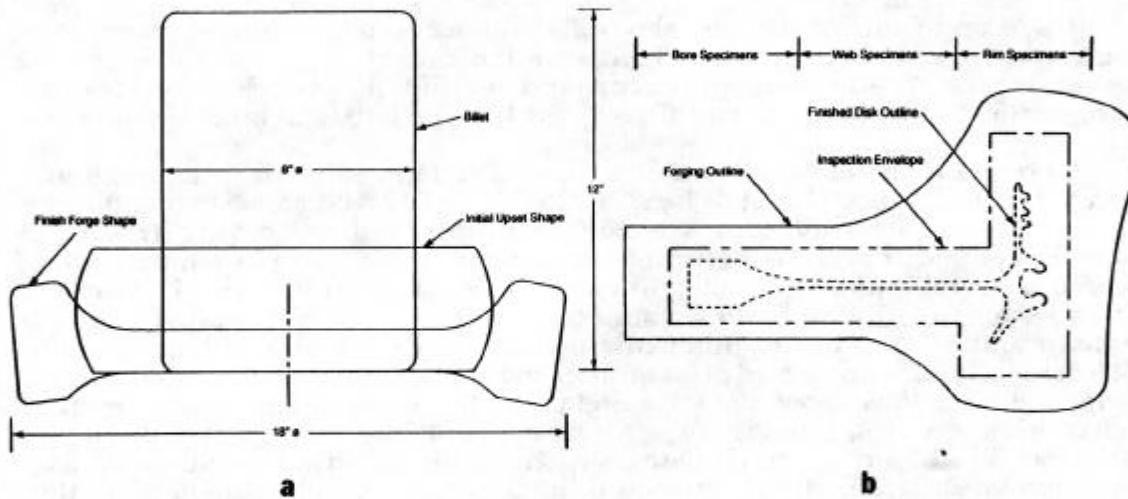


Figure 6 - Schematic drawing of (a) compressor disk two step forging process and (b) finished part and inspection envelope within the forging cross section.

Table IV. Process Conditions for Compressor Disk Forgings

Forging I.D.	Initial Upset		Final Upset		Remarks
	Red. (%)	Temp. (°F)	Red. (%)	Temp. (°F)	
A	60	1875	75	1800	Reference forging
B	60	1875	75	1800	3X transfer time to quench
C	60	1875	75	1800	Aircool after final upset
D	60	1875	75	1850	High final upset temp.
E	70	1875	60	1775	Low final upset temp.
G	80	1875	40	1800	Altered reductions
H	60	1875	75	1800	Coarse grain billet
J	60	1875	75	1800	2X transfer time to press



forging temperature (forgings D and E), furnace-to-press transfer time (forging J), and forging reduction (forging G, and to some extent E). Finally, the input billet multiple for forging H had received a pre-exposure to coarsen the grain size to an average of ASTM 3.

Age treatment of the forgings typically consisted of two standard duplex ages. This procedure was selected since it represents the production practice used for compressor spools. In spool fabrication, fully heat treated forgings are machined for welding and inertia welded together at the rim. A second age treatment for the entire spool is then added to ensure adequate properties in the inertia welded regions.

### Structure

The examination of metallographically prepared macro-sections revealed that good structure uniformity was achieved within the inspection envelope (Figure 6) for all forgings. Die lock areas, however, were still observed in the top and bottom regions of the thinner bore/web area. Figure 7 shows a photograph of a macro-section for the reference forging, A, where the contrast in surface and internal structures is apparent. A microstructural evaluation performed on samples obtained from bore, web and rim areas that would be located within the inspection envelope revealed little variation within each forging. Typical grain structures consisted of fine recrystallized grains, ASTM 11, with some evidence of a slightly finer, more uniform grain size in the thinner bore/web regions. Exceptions were forgings E and H, where a lower finish forge temperature and larger input grain size could be associated with a more common occurrence of unrecrystallized or larger grains, ASTM 3-5 in size. Figure 8 shows optical micrographs of the typical uniform fine grain structure and the more duplex grain structures observed in the rim region of forgings E and H. Metallographic examination also revealed that twin boundaries were not uncommon, and that microstructures from forging E contained more  $\delta$  phase than the other forgings. The larger amount of  $\delta$  in forging E indicates that the 1775°F final upset operation caused some additional precipitation of this phase.

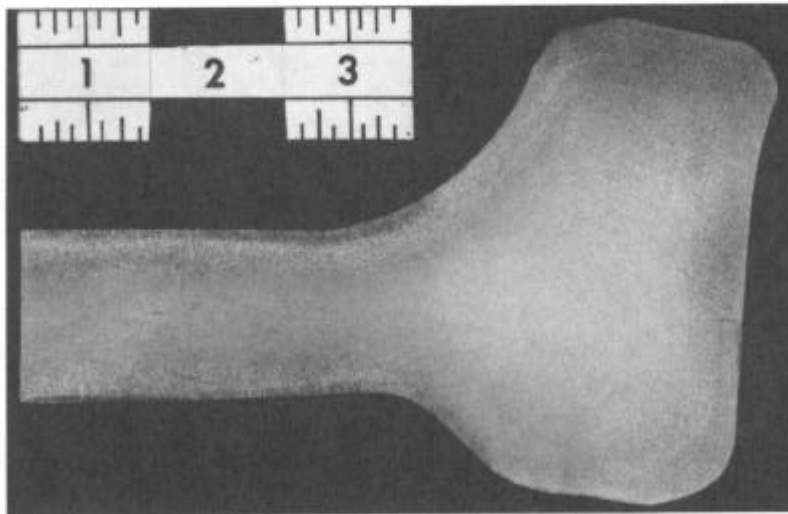


Figure 7 - Photograph of macro-section from compressor disk forging A.

Thin foil and replica transmission electron microscopy (TEM) were used to better characterize the  $\delta$  phase particles and examine the  $\gamma'$  and  $\gamma''$  precipitates of the reference forging. In thin foil studies, the  $\delta$  particles were observed at grain boundaries and within grains, and found to be plate or lath-like in shape.

In some cases, these particles exhibited a preferred crystallographic orientation relationship with the matrix. Although a wide range in size and aspect ratio was observed, the great majority had no dimension greater than about 1  $\mu\text{m}$ . A TEM replica micrograph is shown in Figure 9 to illustrate typical  $\delta$  phase particles. The  $\gamma'$  precipitates are shown in Figure 10 where thin foil dark field images of the  $1/210$  and  $110$  superlattice reflections are used to illustrate two variants of this phase. The  $\gamma'$  precipitates have a disc thickness of 5-15 nm and diameter of 20-40 nm. It should be noted that the  $110$  reflection also contains a  $\gamma'$  contribution. To properly distinguish the  $\gamma'$  particles, a comparison of reflections for the same  $\gamma'$  variant is necessary (3). Following this procedure, the  $\gamma'$  particles were determined to be spherical in shape and typically less than 15 nm in diameter.

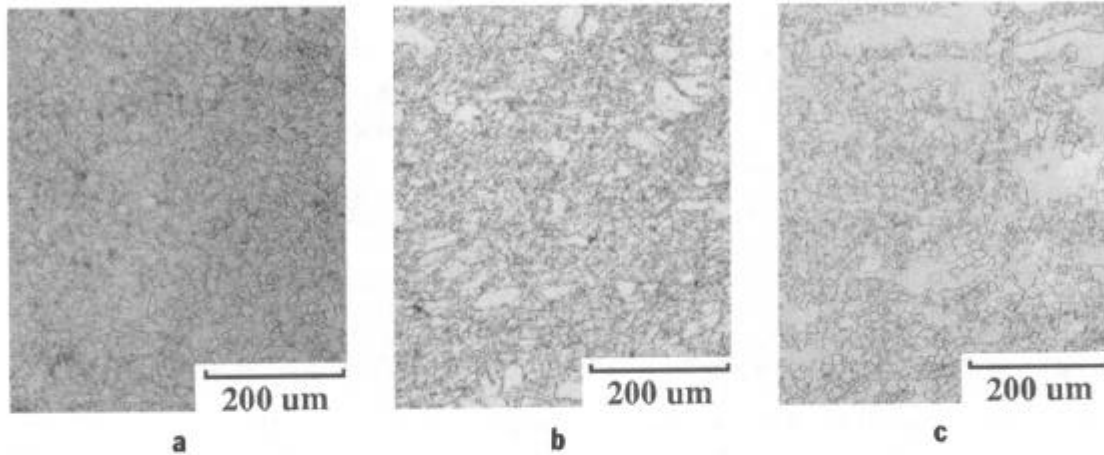


Figure 8 - Rim region microstructures for (a) the "reference disk" A, (b) the "low forge temperature disk" E, and (c) the "coarse grain billet disk" H.

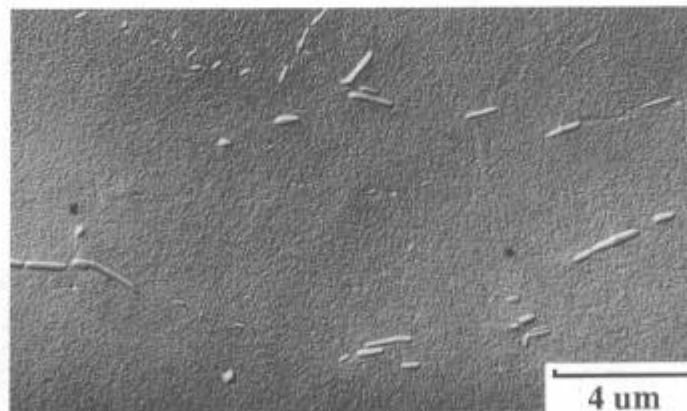


Figure 9 - Typical delta phase particles observed in "reference disk" A.

Figure 11 shows optical and TEM replica micrographs of typical HS718 for comparison with the DA718 compressor disk microstructures. The grain size of HS718 is larger, and more pronounced amounts of lath-like  $\delta$  are present in the structure. The larger grain size results from the use of higher temperatures and lower reductions during forging, while the differences in  $\delta$  phase are primarily due to the use of a sub- $\delta$  solvus solution during heat treatment.

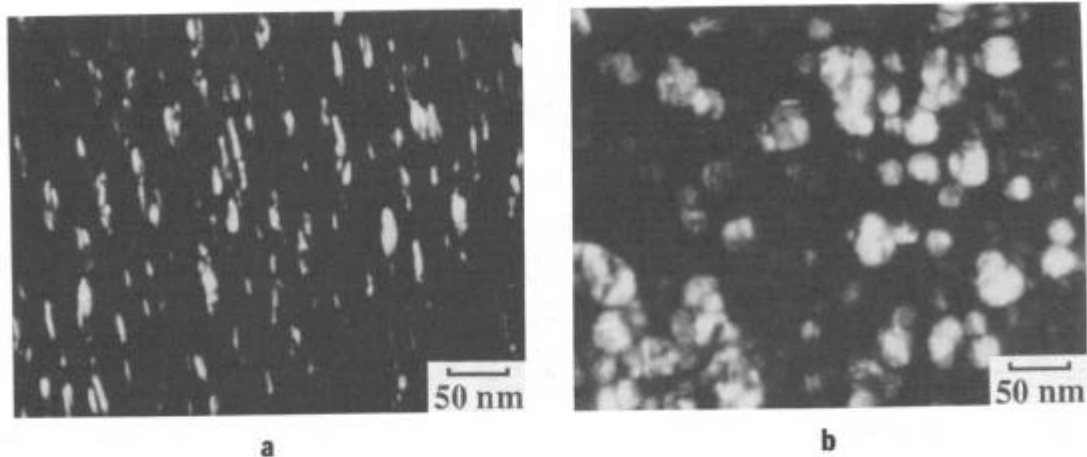


Figure 10 -  $\gamma'$  and  $\gamma''$  precipitates in "reference disk" A; (a) [100]  $\gamma'$  variant,  $g=1/210$ , showing  $\gamma''$  and (b) [001]  $\gamma'$  variant,  $g=110$ , showing  $\gamma'$  and  $\gamma''$ .

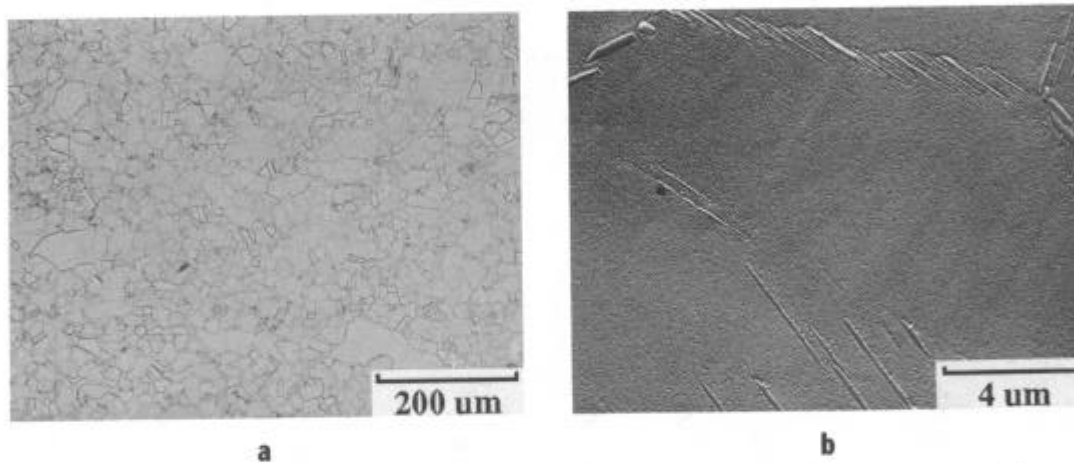


Figure 11 - Microstructure of typical HS718; (a) optical micrograph and (b) TEM replica micrograph.

### Mechanical Property Results

Tensile, creep, LCF, and fatigue crack growth rate (FCGR) tests were performed on the compressor disk forgings to determine the effects of the process variations on mechanical properties. For certain properties, sufficient data was obtained for the construction of average data curves. All specimens and procedures for tensile, creep, and LCF tests were in conformance with accepted ASTM practices. The FCGR tests were conducted using a direct current potential drop method for monitoring crack growth (7). All mechanical property data were obtained from specimens machined with a "tangential" orientation. This orientation represents material subjected to hoop stress loading, the most critical loading direction for disks.

Tensile. Table V lists the tensile results for tests performed at room temperature and 1200°F. All specimens were machined from the bore region. The UTS and YS data show very little variation between the forgings and indicate a high degree of tensile property insensitivity for the process and microstructure variations considered.

Table V. Tensile Properties of Compressor Disks

Forging I.D.	Room Temperature			1200°F		
	UTS (ksi)	YS (ksi)	RA (%)	UTS (ksi)	YS (ksi)	RA (%)
A	213.6	187.8	36.3	178.8	164.0	40.9
B	215.9	191.4	39.7	176.8	159.0	39.6
C	216.4	193.3	38.1	178.3	160.2	46.0
D	217.3	194.3	37.3	177.4	162.5	48.3
E	219.3	195.9	35.1	177.0	162.8	46.0
G	219.1	195.5	36.3	178.6	163.8	42.6
H	218.0	195.6	39.0	177.4	163.0	48.1
J	217.9	195.1	39.1	175.5	161.7	47.9

More extensive tensile testing using specimens machined from regions throughout the forgings continued to show very limited data scatter for the forgings, although specimens from the rim region tended to show lower strength. This is consistent with the larger average grain size observed for this region of the forgings. Figure 12 shows the average tensile strength curves generated for tests performed over the room temperature to 1200°F range. Compared to HS718, the UTS curve is about 10% higher and the YS curve is as much as 20% higher. Tensile reduction in area values for the DA718 tests were found to be similar to, or higher than HS718.

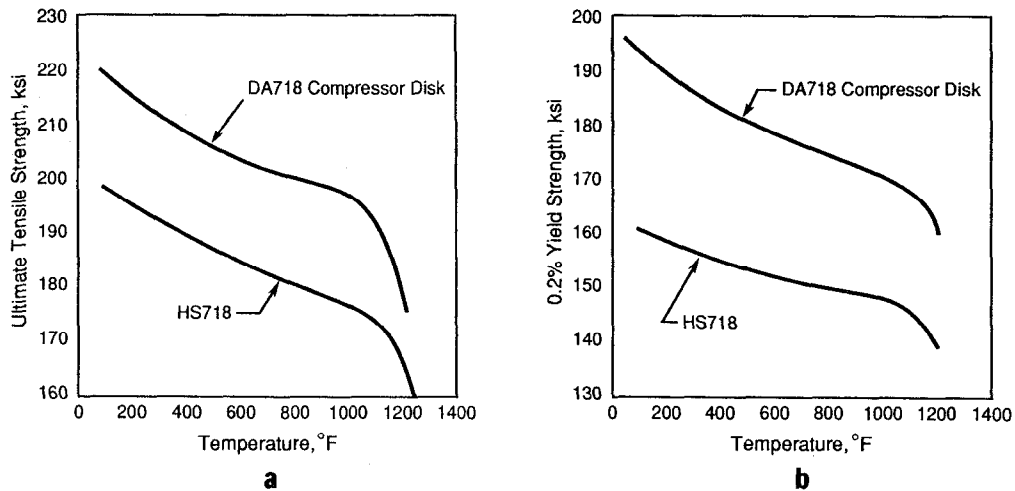


Figure 12 - Tensile data curves for compressor disks; (a) UTS and (b) 0.2% YS.

**Creep.** For an initial comparison of the disk materials, constant load creep testing was performed on specimens from the rim region using a stress of 115 ksi at 1100°F. The time to 0.2% total strain was similar for most of the forgings and ranged from about 1400 to 1900h. Forgings E ("low forge temperature") and H ("coarse grain input billet"), however, exhibited 0.2% creep lives of 235 and 2360h, respectively. Figure 13 shows the specimen microstructures for these two tests, and the microstructure of a specimen with an 0.2% creep life of 1420h. The low result for forging E can be correlated with a larger amount of  $\delta$  phase and some evidence of less recrystallization, while the high result for forging H correlates with the larger grain size of the recrystallized structure.

The results for the 1100°F/115 ksi tests and additional tests performed over the 1000 to 1200°F range are shown in Figure 14. The creep capability of the compressor disk materials is greater than that of HS718 at 1000 and 1100°F, but similar to HS718 at 1200°F. It should be noted that the low 1100°F/115 ksi result for forging E lies on the HS718 1100°F curve, and thus was equivalent to typical HS718 behavior.

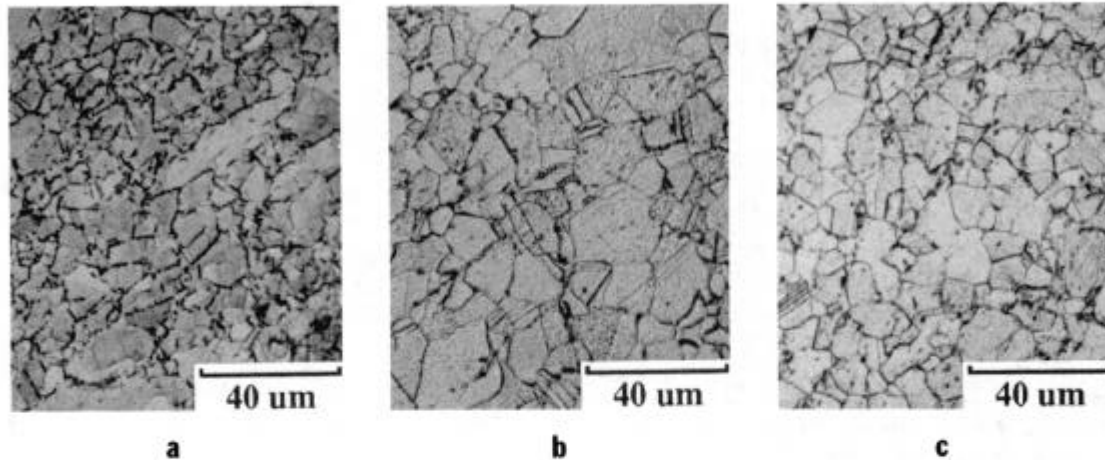


Figure 13 - 1100°F/115 ksi creep specimen microstructures for (a) the "low forge temperature disk" E; low life, (b) the "coarse grain billet disk" H; high life, and (c) a typical disk; intermediate life.

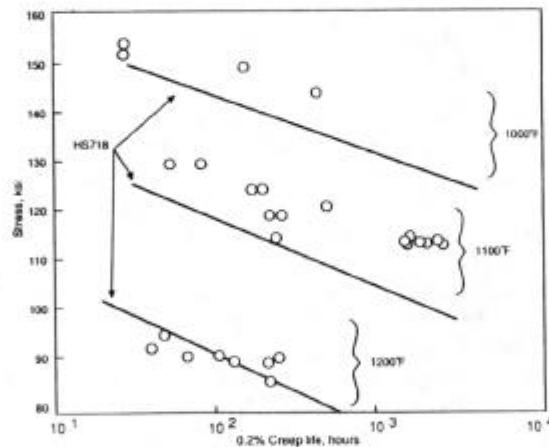


Figure 14 - 0.2% creep life data for compressor disks.

**Low Cycle Fatigue.** Low cycle fatigue testing was conducted over the 300 to 1100°F temperature range using total strain control, a strain A ratio (alternating strain/mean strain) of 1.0, a frequency of 20 cpm, and a triangular waveform. Specimens were machined from forgings selected to survey the range in processing and microstructures (forgings A, B, C, E, J, and H). Consistent with the typical steady state temperature distribution of compressor disks, low temperature (300°F) tests were performed on bore/web material, while high temperature (1000 and 1100°F) tests were performed on rim materials. At 750°F, specimens were obtained from all regions.

The 750°F test results are shown in Figure 15, where the flagged points indicate discontinued tests. It can be seen that the compressor disk data are

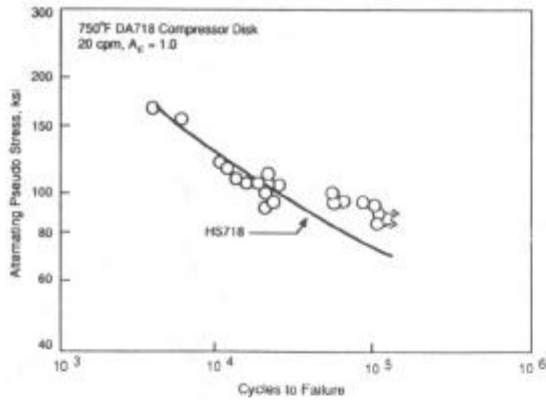


Figure 15 - 750°F low cycle fatigue data for compressor disks.

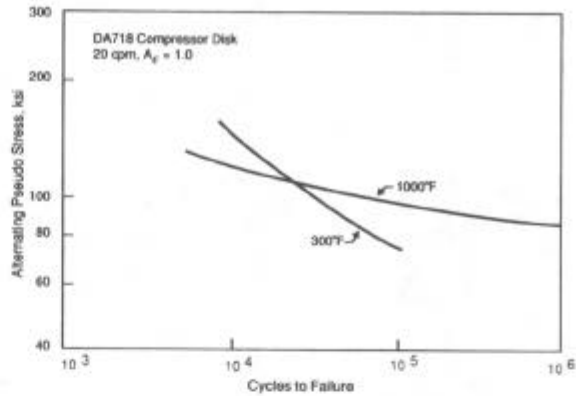


Figure 16 - Low cycle fatigue crossover behavior.

typically similar to the HS718 curve, except in the low pseudostress-long life regime where the DA718 lives are longer. This behavior agrees with the trend shown in Figure 1 for 1000°F DA718 behavior.

A comparison of the results for different temperatures revealed a crossover in LCF life with temperature, consistent with the typical response of Alloy 718 (8). The crossover behavior is shown in Figure 16 where the average curves generated for 300 and 1000°F behavior are presented. Fatigue life at high stress is greater for 300°F tests, while fatigue life at low stress is greater for 1000°F tests.

Microstructures and fracture surfaces of all LCF specimens (nearly 80 tests) were examined to study the effects of grain structure and fatigue initiation site on LCF life. The study of microstructures revealed that lower life could be associated with specimens which more commonly exhibited elongated, unrecrystallized grains. SEM study of the fracture surfaces revealed that a great majority of the failures initiated at the specimen surface where small carbide, nitride, or oxide particles were located. For these types of initiation sites, there was some evidence that life correlated directly with initiation site size. The SEM micrographs of Figure 17 show an example of a typical carbide initiation site. The remaining specimens initiated failure at favorably oriented surface grain sites or, in a few cases, small nicks on the specimen gage. It was also observed that increasing test temperature tended to promote initiation at sub-surface grain sites in the low stress regime. Low test temperature or higher stress levels promoted initiation at surface particle sites.

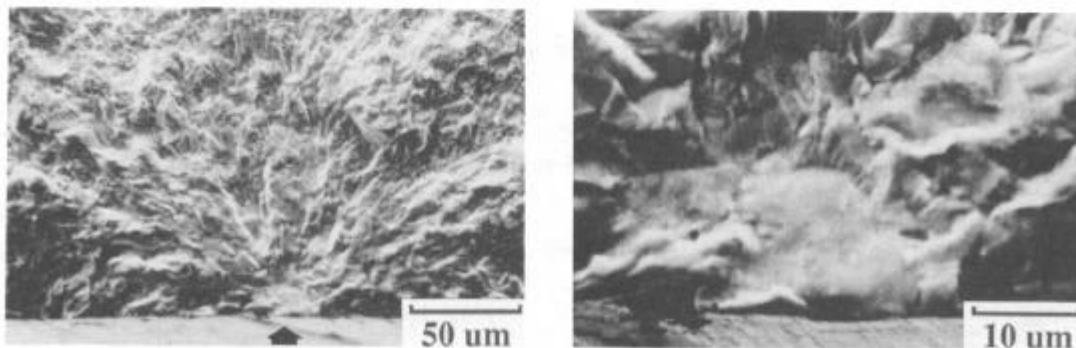


Figure 17 - Typical carbide particle fatigue origin.

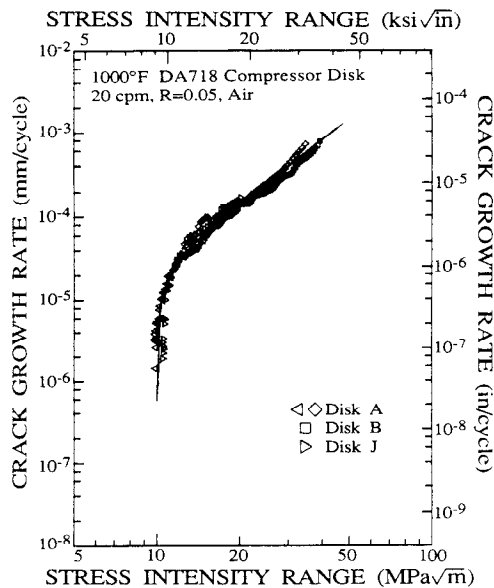


Figure 18 - 1000°F fatigue crack growth rate data for compressor disks.

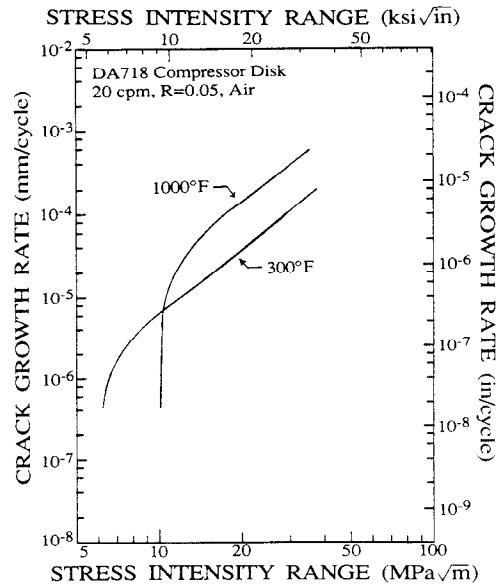


Figure 19 - Fatigue crack growth rate crossover behavior.

**Fatigue Crack Growth Rates.** Rim material from the reference forging and forgings B ("delay to quench") and J ("low forge temperature") were selected for the first DA718 FCGR tests. A direct current potential drop technique was used to monitor the crack growth from small semicircular or chord-shaped flaws electrical discharged machined on the surface of cylindrical gage LCF specimens. The specimens and test procedures are described in more detail elsewhere (7). It should be noted that the near-threshold data for this test technique are obtained in load control tests by systematically step-loading the specimen until initiation and growth occurs. These data may thus not represent true behavior, but for identical flaw geometries are suitable for comparison and the study of behavioral trends. Results from this test technique have been shown to be consistent with those from the more advanced techniques currently used at GEAE today.

Based on the results obtained for several temperatures, no significant or consistent differences in FCGR were observed for the three forgings. Figure 18 shows the FCGR data for tests at 1000°F, where the line through the data represents an estimate of the average rates. A similar procedure was used to construct a curve for 300°F results, and Figure 19 shows the FCGR crossover that occurs when curves for both temperatures are compared. At low values of  $\Delta K$ , growth rates at 300°F exceed those at 1000°F, while at high  $\Delta K$  levels, the 1000°F growth rates exceed those at 300°F. This crossover was later confirmed in an investigation which used improved methods to determine near-threshold behavior (9), and has been observed in HS718 and other disk materials (10). The subsequent investigation (9) concluded that the FCGR crossover is most likely due to localized crack tip blunting, rather than closure or deformation mode effects. It was also shown that the LCF crossover could be rationalized from the crossover in FCGR.

SEM study of the crack path morphology for specimens tested at 300 and 1000°F revealed that the fracture mode was predominantly transgranular at both temperatures, although some evidence of occasional intergranular fracture was observed for the 1000°F tests. Figure 20 shows the typical 300 and 1000°F morphology for an intermediate  $\Delta K$  level.

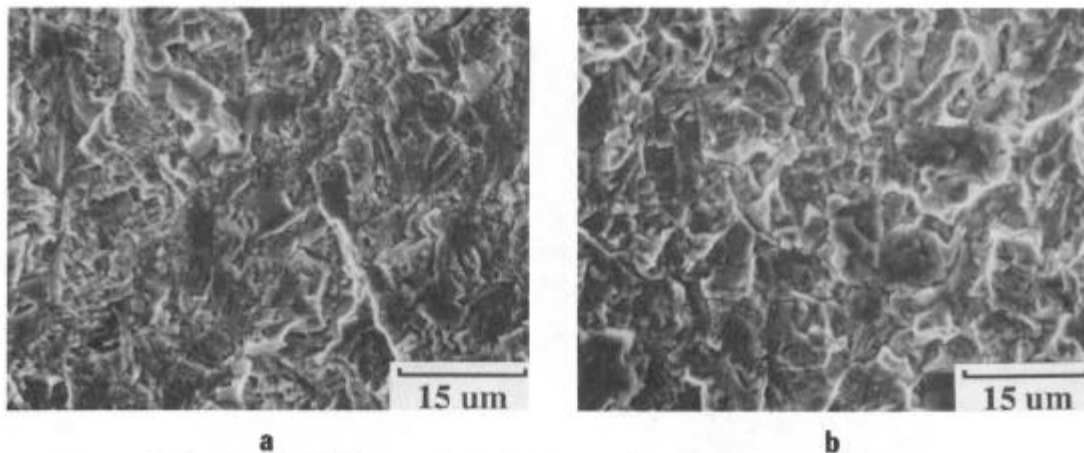


Figure 20 - Typical fatigue morphology of compressor disk crack growth specimens at (a) 300°F and (b) 1000°F.

### Aging Response

The isothermal aging behavior of the compressor disk materials was studied over the 1100 to 1350°F range. As-forged samples from similar bore locations were exposed for periods up to 24h, metallographically prepared, and evaluated for average vickers diamond pyramid hardness (VDPH) using a 10kg load. The average and range in results for the forgings at each aging condition are compared with "as-forged" results in Figure 21. The general behavior shown in this figure represents classical aging response, characteristic of Alloy 718 (11). Hardening occurs more rapidly as aging temperature is increased, and these DA718 materials show peak hardening in the 1250-1300°F regime. For low temperature aging, the range in hardness response for the forgings is much larger than that for the higher temperatures. This was largely due to a significantly higher hardness for forging C ("air cooled"). In the as-forged condition, the sample from this forging had a hardness of 363 VDPH, while the other forgings ranged from 271 to 296 VDPH. This suggests that the air cool after the final upset resulted in some initial precipitation strengthening. The samples from forgings E ("low forge temperature") and G ("altered reduction ratio") also tended to show more a more rapid aging response, but the reasons for this are not clear.

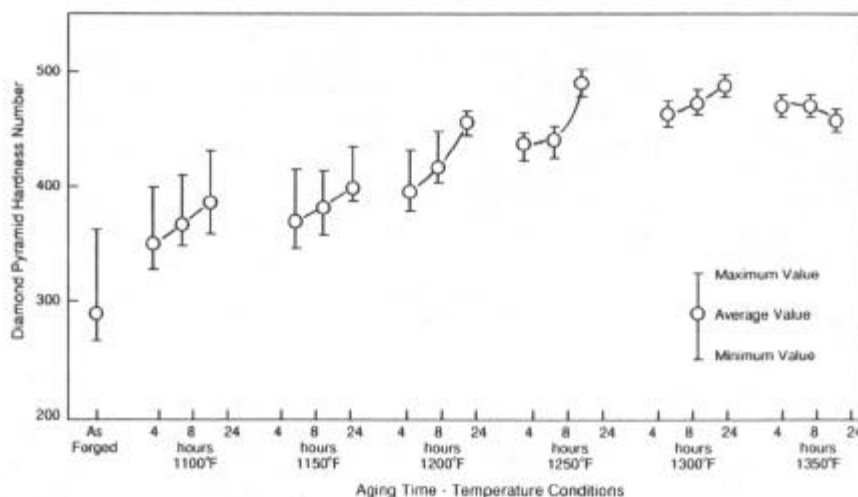


Figure 21 - Hardness-time aging behavior of compressor disk materials.



Another part of the aging study included a comparison of bore region tensile properties for the compressor disk materials after a double standard duplex age (appropriate for compressor spools), a single standard duplex age (appropriate for other potential disk applications), and the typical HS718 heat treatment: 1775°F/1h/water quench plus standard duplex age. The average UTS and YS results for specimens with a double duplex age were 217 and 194 ksi, respectively (the data for these tests are shown in Table 5). Specimens with a single duplex age showed slightly higher strengths, and had average UTS and YS values of 220 and 198 ksi, respectively. Subsequent TEM thin foil studies on DA718 materials (12) have shown that the  $\gamma''$  precipitate size is increased for a double duplex age, and this may be related to the slight difference in strength. Although only several tests were performed for the HS718 heat treatment, the UTS and YS capability of DA718 was clearly diminished. Average UTS and YS values were 210 and 170 ksi, respectively. Very careful structure and phase characterization experiments would be required to fully explain the loss in strength for this heat treatment. It is most likely due to some depletion of the  $\gamma'$  and  $\gamma''$  precipitates which would occur with an increase in the amount of  $\delta$ , along with possible changes in the substructure.

### Discussion

Evaluation of the trial compressor disk materials showed that the Direct Age process would result in improved properties for full-scale Alloy 718 disks. Compared to HS718, UTS and YS properties over the room temperature to 1200°F range were about 10 and 20% higher, respectively, while creep and LCF properties were at least equivalent, and even greater under certain conditions. Although careful control of the process is necessary, the low data scatter for the compressor disk forging variations indicated a satisfactory degree of process tolerance. Process-structure-property correlations revealed that the best combination of tensile, creep, and low cycle fatigue properties was obtained from a uniform, fine, recrystallized grain size with minimal  $\delta$  phase. Other investigations also showed a crossover in FCGR behavior, demonstrated the classical aging reponse of Alloy 718, and determined that the tensile strength of DA718 would be lower if the standard solution plus duplex age was used for heat treatment.

### Summary

Through the evaluation of trial pancake and compressor disk forgings, the Direct Age process was successfully developed and applied to a full-size Alloy 718 disk configuration. This process makes use of high forge reductions at lower temperatures and an age only heat treatment to achieve improved disk properties. The process iterations during the pancake and compressor disk trials revealed the need to control the grain size throughout the process and use forging temperatures above the  $\delta$  solvus. As a result of this work and follow-on full-scale implementation programs, DA718 is presently used for the high pressure turbine disk, one disk type seal, and six individually forged compressor disks in an advanced commercial engine. Further process refinement has led to the use of isothermal forge conditions and more sophisticated die configurations to improve microstructure uniformity throughout the disks, eliminate die-chill regions, and achieve near-net shapes.

### Acknowledgments

The GEAE Direct Age 718 development effort was performed under the direction of Mr. J. F. Barker, and Mr. D.M. Carlson was responsible for much of the initial work. It is also appropriate to recognize the efforts of the Wyman Gordon Company where key contributions during the trial forging programs were made by Mr. W. H. Coutts and Mr. K. Kolstrom. The transmission electron microscopy was performed by Dr. E. L. Hall of GE Corporate Research and Development. Technical support was provided by many personnel at GEAE. The efforts of Mr. W. V. Ross warrant special recognition.

### References

1. J. F. Barker, D. D. Krueger, and D. R. Chang, *Advanced High Temperature Alloys: Processing and Properties* (Metals Park, OH: American Society for Metals, 1986), 125-137.
2. J. M. Oblak, D. F. Paulonis, and D. S. Duvall, "Coherency Strengthening in Ni-Base Alloys Hardened by DO<sub>22</sub>," *Journal of Metals*, (Oct.)(1969), 34-38.
3. D. F. Paulonis, J. M. Oblak, and D. S. Duvall, "Precipitation in Nickel-Base Alloy 718," *Transactions of the ASM*, 62 (1969), 611-622.
4. R. Cozar and A. Pineau, "Morphology of  $\gamma'$  and  $\gamma''$  Precipitates in Nickel-Base Alloy 718," *Metall. Trans.*, 4 (1973), 47-59.
5. I. Kirman and D. H. Warrington, "The Precipitation of Ni<sub>3</sub>Nb Phases in a Ni-Fe-Cr-Nb Alloy," *Metall. Trans.*, 1 (1970), 2667-2675.
6. W. H. Coutts, unpublished research, Wyman Gordon Company, North Grafton, Massachusetts.
7. R. H. Van Stone, D. D. Krueger, and L. T. Duvelius, *Fracture Mechanics: Fourteenth Symposium-Volume II: Testing and Applications*, ASTM STP 791 (Philadelphia, PA: American Society for Testing and Materials, 1983), II553-578.
8. T. H. Sanders, Jr., R. E. Frishmuth, and G. T. Embly, "Temperature Dependent Deformation Mechanisms of Alloy 718 in Low Cycle Fatigue," *Metall. Trans. A*, 12A (1981), 1003-1010.
9. R. H. Van Stone and D. D. Krueger, "Investigation of Direct Aged Inconel 718 Fatigue Behavior" (Final Report: NAVAIR Contract N00019-82-C-0373, GE Aircraft Engines, Cincinnati, Ohio, 1984).
10. D. D. Krueger, unpublished research, GE Aircraft Engines, Cincinnati, Ohio.
11. M. Kaufman and A. E. Palty, "The Phase Structure of Inconel 718 and 702 Alloys", *Transactions AIME*, 221 (1961), 1253-1262.
12. E. L. Hall, unpublished research, GE Corporate Research and Development, Schenectady, New York.